Fractional revival "matrix mechanics" in quantum billiards

Bernd Rohwedder
Hauptstrasse 47, 67059 Ludwigshafen, Germany
(Received 3 April 2008; published 21 July 2008)

Certain classes of integrable quantum billiards provide a versatile arena for time-domain atom optics experiments. In order to learn how to fully exploit the fractional revival behavior that governs these kinds of systems, we here develop a convenient theoretical framework for their description. As an illustrative example, we present a billiard-internal realization of Grover's quantum search algorithm. The considered devices are scalable and could be used for the construction of quantum computers using trapped neutral atoms.

DOI: 10.1103/PhysRevA.78.012340 PACS number(s): 03.67.Lx, 37.10.Gh, 37.25.+k, 42.25.−p

I. INTRODUCTION

Wave-billiard spectra have attracted considerable attention during the past decades. Exact analytic solutions of the eigenvalue problem have been found in a few exceptional systems only. More typically, information is extracted from the statistical properties of the state density distribution. The study of certain two-dimensional polygonal enclosures has led to a natural generalization of the concept of billiard integrability [1]. Higher-dimensional polyhedra enclosures have also been mathematically analyzed [2]. For geometries that are known to lead to chaos in the ray-optics ("classical") limit the questions arise; if and in which sense the same concept is also applicable to the wave-optics ("quantum") versions of these systems [3]. Experiments have been conceived to test the diverse predictions. Microwave billiards can be employed to simulate the de Broglie wave dynamics in a macroscopic frame [4]. Electrons trapped in semiconductor billiards, on the other hand, have been used to study chaos-related issues in the quantum domain [5]. Similar studies have taken place with atoms confined in two-dimensional corrals made of light [6]. However, in these latter experiments the accessible parameter space has so far not allowed the observation of specifically wavelike features, i.e., the dynamics could be essentially understood in classical terms.

In view of these fascinating developments, it is understandable that integrable (wave-)billiards are perhaps generally considered to be less interesting objects of study. The main goal of this paper is to demonstrate that there nevertheless exist quite noteworthy objects among these systems, which in our opinion deserve special attention as well. By developing a conveniently adapted theory for their description, we are able to discuss how they could be used for both classical and quantum computing purposes. The rather unique feature which makes this possible is the fact that in this class of systems, the introduction of a proper ("stroboscopic") observation-time discretization leads also to a discrete (spatial) wave packet evolution, in a sense to be defined later. Fractional revivals are the key to this phenomenon. For a recent review, see Ref. [7]. Since we believe that our results may turn out to be most valuable in the quantum domain, in this paper we will often be referring to "quantum" billiards. It should nevertheless always be kept in mind that the essence of the problem treated here is linked to wavelike behavior in general and not to anything specifically "quantum."

The paper is structured as follows. After this introduction, we first specify how and under which circumstances the dynamics in a quantum billiard in one, two, or three dimensions becomes intrinsically periodic. Section III then specializes on rectangular (two-dimensional) systems and develops a compact mathematical description of their behavior. The so called "A4 billiard" [8] is then analyzed in more detail and shown to present particular features which allow one to produce, in its interior, arbitrary states of a suitably chosen four-dimensional (discrete) Hilbert space. After demonstrating how a billiard-analog of Grover's quantum search algorithm could be implemented within this frame, the section then proceeds to analyze the scalability properties of nested billiard setups. Proposals for multiple-path ("time-domain atom chip") interferometers, quantum computers with individually trapped neutral atoms, and miniature conveyor belts ("atomic bucket brigades") round up this main part of the paper. After the final Conclusions section, two appendices have been added in order to place the previous results into a broader context. Appendix A first explains how the close relationship with certain self-imaging phenomena in classical optics comes about. Appendix B then closes by using a rather elementary physical argument to derive a mathematical relationship that plays a central role in number theory.

II. TIME-PERIODIC QUANTUM BILLIARDS

In our present context, by a "quantum billiard" we mean a finite and field-free region of one-, two-, or three-dimensional space that has well-defined boundaries and in the interior of which we assume a quantum particle to be confined in such a way that its wave function vanishes on them at all times.

A. The one-dimensional case

The quantum behavior of a particle (mass $\mathcal{M}$) that is one-dimensionally (x axis) trapped in an infinite square well (width a_x) is a standard situation used to illustrate (and solve) Schrödinger's time-dependent and time-independent equations in many introductory textbooks. It is worth noticing, however, that most discussions come to a halt as soon as the eigenfunction expansion has been written down. At the very best, some numerical examples of wave packet evolution are pictorially represented.

It seems almost unknown that this problem allows an explicit closed solution which is independently valid for any possible initial condition. Since this solution will be our workhorse in the next section, we are now going to present a concise derivation. It is our hope that the simplicity of the approach will induce readers to incorporate this neat (and not at all novel; see, for instance, Ref. [9]) result in elementary quantum mechanics lectures.

We first introduce the natural time scale $T \equiv 4\mathcal{M}a_x^2/(\hbar\pi)$. It is convenient then to define rationalized space and time coordinates according to $\xi \equiv \pi x/a_x$ and $\tau \equiv 2\pi t/T$. If the origin of the coordinate system is chosen symmetrically with respect to the potential walls, the rationalized and normalized energy eigenfunction of order μ ($\mu = 1,2,3,\ldots$) will be given by

$$\psi_\mu(\xi) = \sqrt{\frac{2}{\pi}} \sin\left[\left(\xi + \frac{\pi}{2}\right)\mu\right], \tag{1}$$

where the restriction $|\xi| \leqslant \pi/2$ is tacitly understood. The time propagation of an arbitrary state

$$\psi(\xi,\tau) = \sum_{\mu=1}^{\infty} c_\mu \psi_\mu(\xi) e^{-i\mu^2\tau}, \tag{2}$$

where c_μ are expansion coefficients. By substituting τ by $\tau + 2\pi$, one immediately verifies that the temporal behavior is periodic: $\psi(\xi,\tau+2\pi) = \psi(\xi,\tau)$. This identifies T as a characteristic revival time of the one-dimensional quantum box problem [7].

One can go further by analyzing the situation at fractional multiples of the revival time, $\tau = 2\pi m/n$, where m and $n \neq 0$ are integers. Since the phase factor $\exp(-i2\pi\mu^2 m/n)$ is n periodic with regard to μ, it can be harmonically expanded [10],

$$\exp\left(-i2\pi\mu^2\frac{m}{n}\right) = \sum_{\mu'=1}^{n} C(\mu',m,n)\exp\left(i2\pi\frac{\mu\mu'}{n}\right), \tag{3}$$

where the Fourier coefficients

$$C(\mu',m,n) \equiv \frac{1}{n}\sum_{s=1}^{n} \exp\left(-i2\pi\frac{ms^2+\mu's}{n}\right) \tag{4}$$

are Gauss sums, known as "Talbot coefficients" in the optics literature (see Appendices A and B). Since the left-hand side of Eq. (3) is an even function of μ, we can rewrite

$$\exp\left(-i2\pi\mu^2\frac{m}{n}\right) = \sum_{\mu'=1}^{n} C(\mu',m,n)\cos\left(2\pi\frac{\mu\mu'}{n}\right) \tag{5}$$

and introduce this expression together with eigenfunction (1) into Eq. (2). The trigonometric identity $2\sin\alpha\cos\beta = \sin(\alpha+\beta)+\sin(\alpha-\beta)$ can then be used to obtain

$$\psi\left(\xi, 2\pi\frac{m}{n}\right) = \sum_{\mu'=1}^{n} C(\mu',m,n) \times \sum_{\mu=1}^{\infty} c_\mu \frac{\psi_\mu(\xi+2\pi\mu'/n) + \psi_\mu(\xi-2\pi\mu'/n)}{2}, \tag{6}$$

where Eq. (1) has been reintroduced twice. The restriction $-\pi/2 \leqslant \xi \leqslant \pi/2$ has not so far played any role and it is, at this point, notationally practical to lift it completely by generalizing the range of Eq. (1) to arbitrary ξ. By doing so, the wave function becomes both spatially periodic, $\psi(\xi,\tau) = \psi(\xi+2\pi,\tau)$, and odd (with respect to the box borders), $\psi(\pm\pi/2+\xi,\tau) = -\psi(\pm\pi/2-\xi,\tau)$. Equation (6) can now be written

$$\psi\left(\xi, 2\pi\frac{m}{n}\right) = \sum_{\mu'=1}^{n} C(\mu',m,n) \times \frac{\psi(\xi+2\pi\mu'/n,0) + \psi(\xi-2\pi\mu'/n,0)}{2}, \tag{7}$$

which is a finite expression involving only stepwise laterally shifted copies of the initial (given) wave function and corresponding weighting factors. Such superpositions are known as "fractional revivals" of a wave function.

This is a noteworthy and truly exceptional result. Usually, the time development of an arbitrary wave function is expressed in terms of an integral propagator. [Consult Ref. [11] for the propagator corresponding to the present case and its relation to Eq. (7)]. Even in the simple case of a completely free particle in one dimension, the integration step cannot be skipped. Equation (7), on the other hand, expresses that this is quite different in the present situation, where a universal temporal behavior is obtained. This unique property indeed identifies the box problem as the most elementary *mechanical* system of quantum physics. The connection between quantum revivals and classical periodicity is pedagogically presented in Ref. [12].

B. The two-dimensional case

Due to the separability of the resulting problem, it is immediately obvious that rectangular billiards can lead to periodic revival phenomena as well. If a_x and a_y denote the side lengths of a rectangular billiard and we choose to place its center at the origin of our coordinate system, then all eigenfunctions are obtained by merely multiplying the one-dimensional version (1), evaluated at $\xi = \pi x/a_x$, by the analogous expression evaluated at $\eta \equiv \pi y/a_y$. Whenever there exist two natural numbers M and N such that $(a_x/a_y)^2 = M/N$, the resulting system evolution will be periodic with a revival time equal to

$$T \equiv \frac{4\mathcal{M}}{\hbar\pi} a_x a_y \sqrt{MN}. \tag{8}$$

In order to make sure that this is the minimal period of the system, the fraction M/N must be irreducible. By measuring t again in these units, $\tau = 2\pi t/T$, one obtains the analog of Eq. (2), i.e.,

$$\psi(\xi,\eta,\tau) = \sum_{\mu=1}^{\infty}\sum_{\nu=1}^{\infty} c_{\mu\nu}\psi_\mu(\xi)\psi_\nu(\eta)e^{-i(N\mu^2+M\nu^2)\tau}. \tag{9}$$

In the particular case of a square billiard, due to the degeneracy caused by the special condition $a_x = a_y$, it becomes possible to linearly combine degenerate eigenfunctions in such a way, that the resulting superposition vanishes on the billiard diagonals. From this it is clear, and it has long been known, that also a billiard in the shape of a (rectangular) isosceles triangle can be "solved." Only in 1980 it was discovered, in two nearly simultaneous papers [13,14], that also the eigenfunction system belonging to an equilateral triangular billiard involves but products of elementary trigonometric functions. This result is one of the rather rare examples of a nonseparable problem for which the exact analytical solution has been found. The completeness of the identified eigenfunction set was rigorously proved a few years later [15]. By considering solutions that vanish on the line that symmetrically bisects the equilateral triangle into a pair of rectangular ones, the resulting 30°-60°-90° triangular billiard shape can also be completely (analytically) tackled.

The emergence of quantum revivals in the (rectangular) isosceles triangle is a direct consequence of the corresponding property of its square ($M/N=1$) progenitor. Quantum revivals in equilateral triangles (and their symmetric halves) have been thoroughly studied in Ref. [16]. The question quite naturally arises, if there exist also other geometrical shapes capable of producing periodic quantum revivals of an *arbitrary* initial wave function. One could for instance be led to think that the rhombus obtained by gluing two equilateral triangles together would produce such revivals. This, however, is not the case. For the set of eigenfunctions obtained by multiplying the two equilateral triangle eigenfunction sets is not complete, inasmuch as only odd-symmetry solutions (under reflection about the short diagonal) are obtained. The other exact half of the set, consisting of the even-symmetry solutions including the ground state, cannot be generated this way [17]. Also the hexagon [18] and all other geometrical figures that can be created by such a gluing procedure do *not* lead to intrinsically periodic quantum dynamics [19]. In 1991 it was shown that besides the already mentioned examples, no other billiard shapes are amenable to solution in terms of trigonometric function products [20]. A rigorous no-go theorem has been formulated and proved in Ref. [21]. One concludes that time-periodic two-dimensional quantum billiard systems are restricted to the special cases mentioned so far.

C. The three-dimensional case

From what has been said, it becomes immediately clear that any prism along the z axis will have eigenfunction systems that can be completely expressed in terms of simple trigonometric function products *as long as* the prism profile is either shaped similar to a rectangle or like one of the three triangles 60°-60°-60°, 45°-45°-90°, or 30°-60°-90°. If, in addition, the time period corresponding to a certain prism length (z axis) is compatible with the transverse (x-y plane) period of a given profile figure, the resulting temporal behavior of the prism billiard will be periodic itself. The author is not aware of the existence of any further billiards in three dimensions sharing these characteristics.

III. QUANTUM BILLIARD ATOM OPTICS

The dynamics described by Eq. (7) are quite complex and rich [22]. It is the main purpose of this paper first to sift out those simple enough features that could turn out to be useful for applications and, second, to cast them into a more convenient mathematical form. It is our conviction that if systems with such a unique time behavior do theoretically exist, then it would be foolish not trying to make practical use of them.

Atom optics provides a means to experimentally realize quantum billiards under particularly clean conditions. The realization of a one-dimensional atom billiard with walls made of near-resonant laser light was proposed by Wilkens *et al.* in [23]. A three-dimensional billiard atom "trap" in the shape of a hexaedric box had been proposed even earlier [24]. However, the first actual demonstration of atom billiards took place in two dimensions [25,26].

There exist several optical means to realize both the ideally flat ("quasi-two-dimensional") billiard surface [27–29] and variously shaped billiard walls [29–31] for atoms. To date, experiments with these billiards have concentrated on chaos-related questions in the quasiclassical regime [32]. By employing lighter atomic species in smaller-sized confinements, chaos could also be studied in the quantum domain [8].

It is this quantum domain in two dimensions which will concern us exclusively. However, here we will be dealing with the perfectly regular dynamics in the interior of rectangular billiards with rational aspect ratios

$$\left(\frac{a_x}{a_y}\right)^2 = \frac{M}{N}, \tag{10}$$

as defined in Sec. II B. By doing so, we extend the original proposal made in Ref. [8] to quite arbitrary situations and introduce a superior—highly pictorial—algebraic formalism for its description. Inasmuch as the detrimental effects caused by wall imperfections (real-life billiard cushions are never ideally hard nor are they inifinitely high) have already been considered in [8] and shown to be rather unproblematic under realistic experimental conditions, here we will neglect them entirely.

The thick-bordered square in Fig. 1 represents the billiard under scrutiny. Due to the chosen rationalization of spatial variables, physical billiards of any aspect ratio appear as squares. If an arbitrary initial ($\tau=0$) wave function is symbolically represented by the letter "F," the actual (i.e., natural) spatial period of the problem doubles the billiard lengths

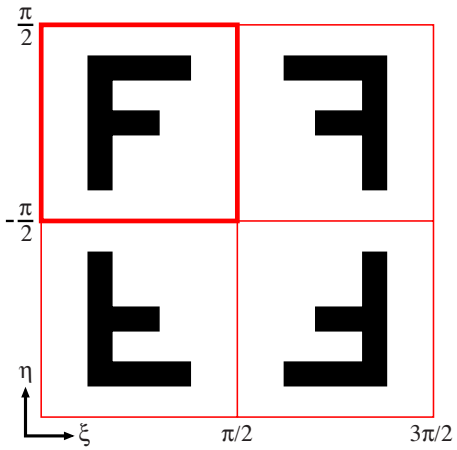

FIG. 1. (Color online) When represented in terms of the rationalized units defined in the main text, a rectangular billiard assumes a square shape (thick lines). Its dynamics can be most easily expressed by extending the considered view into both spatial directions, ξ and η. In order to illustrate the symmetry properties of the billiard wave function in the resulting additional fields (thin lines), we consider an amplitude distribution in the shape of a letter "F."

both along ξ and along η. The correspondingly mirrored images of the initial wave function are also shown in the figure. In order to study the time development, we again begin by considering rational multiples,

$$\tau = 2\pi\frac{m}{n}, \tag{11}$$

of the revival period 2π. We then evaluate Eq. (9) at these times and introduce identity (5) twice. As in Eq. (6), the finite sums (with counter variables labeled μ' and ν') can be extracted and one obtains

$$\psi\left(\xi,\eta,2\pi\frac{m}{n}\right) = \sum_{\mu'=1}^{n}\sum_{\nu'=1}^{n} C(\mu',Nm,n)C(\nu',Mm,n) \times \sum_{\mu=1}^{\infty}\sum_{\nu=1}^{\infty} c_{\mu\nu}\psi_\mu(\xi)\psi_\nu(\eta)\cos\left(2\pi\frac{\mu\mu'}{n}\right) \times\cos\left(2\pi\frac{\nu\nu'}{n}\right). \tag{12}$$

Following the same reasoning that eventually led to Eq. (7), the double infinite series can be rewritten in terms of appropriately shifted copies of the initial wave function and we arrive at

$$\psi\left(\xi,\eta,2\pi\frac{m}{n}\right) = \sum_{\mu'=1}^{n}\sum_{\nu'=1}^{n} C(\mu',Nm,n)C(\nu',Mm,n) \times\frac{1}{4}\left\{\psi\left(\xi+2\pi\frac{\mu'}{n},\eta+2\pi\frac{\nu'}{n},0\right) + \psi\left(\xi+2\pi\frac{\mu'}{n},\eta-2\pi\frac{\nu'}{n},0\right) + \psi\left(\xi-2\pi\frac{\mu'}{n},\eta+2\pi\frac{\nu'}{n},0\right) + \psi\left(\xi-2\pi\frac{\mu'}{n},\eta-2\pi\frac{\nu'}{n},0\right)\right\}. \tag{13}$$

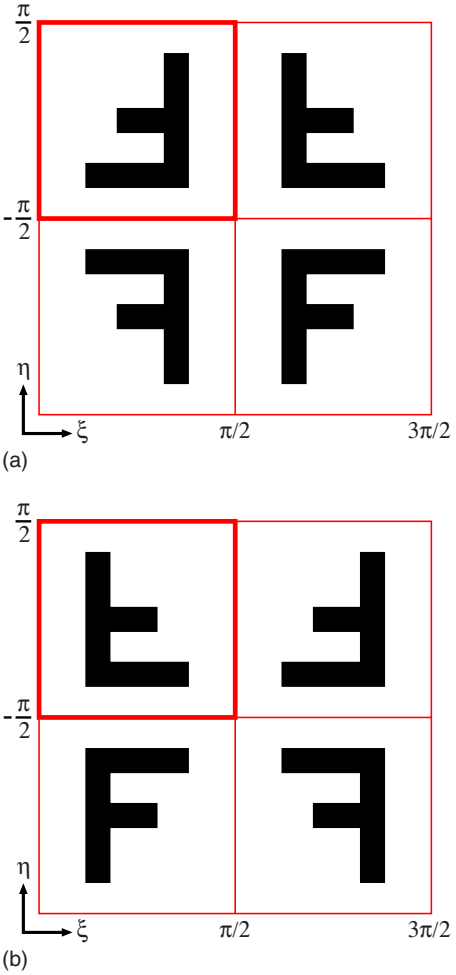

FIG. 2. (Color online) If the situation depicted in Fig. 1 represents the state of the system at the initial time $\tau=0$, then the posterior evolution of the wave function depends on the aspect ratio of the considered billiard. Here we depict the situation at the instant $\tau=\pi$ for the cases $M=1$, $N=1$ (a) and $M=1$, $N=2$ (b).

We illustrate this result with the elementary examples depicted in Fig. 2. They correspond to the time instant $\tau=\pi$. Figure 2(a) represents the situation of a square, $M/N=1$. Using the ingredients $C(1,1,2)=1$ and $C(2,1,2)=0$, one verifies $\psi(\xi,\eta,\pi)=\psi(\xi+\pi,\eta+\pi,0)$. Similarly, case 2(b) refers to a billiard with $M/N=1/2$. Here, also the identities $C(1,2,2)=0$ and $C(2,2,2)=1$ are needed and one can readily check that $\psi(\xi,\eta,\pi)=\psi(\xi,\eta+\pi,0)$. The periodicity relation

$$C(r,m+n,n) = C(r,m,n) \tag{14}$$

is a direct consequence of definition (4). From it we can conclude that Fig. 2(a) applies whenever both M and N are odd, while Fig. 2(b) always applies for odd M and even N. A third—not depicted—situation is obtained if M is even and N

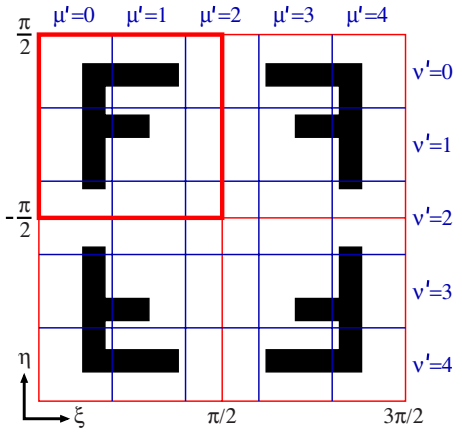

FIG. 3. (Color online) The "sliding tile puzzle" behavior shown in Fig. 2 for the case $m=1$, $n=2$ suggests that the (extended) billiard plane should be conveniently divided into $n\times n$ elementary "tiles" or cells. The procedure and the introduced nomenclature is illustrated in the present figure for the example $n=5$.

is odd. Under these conditions, one computes $\psi(\xi,\eta,\pi)=\psi(\xi+\pi,\eta,0)$. [The possibility that both M and N are even leads to $\psi(\xi,\eta,\pi)=\psi(\xi,\eta,0)$. This is expected, since the fraction M/N in that case is manifestly reducible by a common factor of 2, so that according to Eq. (8) a correspondingly halved period T is obtained.] This classification of all possible dynamic alternatives is possible at any given time instant m/n. Due to the n periodicity expressed by Eq. (14), no more than n^2 different alternatives may exist.

Figure 2 visualizes how the fractional revival dynamics described by Eq. (13) causes whole sections of billiards to be shifted around as in a sliding tile puzzle. If T is divided into n equal time intervals, it is thus natural to cut up the "object" (the wave function distribution in the billiard) into $n\times n$ square pieces. We therefore introduce an "object matrix" ${}_{(n)}\Psi$, the elements ${}_{(n)}\Psi_{\mu',\nu'}$ of which are precisely those individual pieces of the wave function, as representatively shown in Fig. 3 for the case $n=5$. The cyclic (or anticyclic) rotation of the picture's rows and columns along the two axes, as observed in Fig. 2, is then mathematically described by corresponding rotation matrices ${}_{(n)}(\uparrow)$, ${}_{(n)}(\downarrow)$ (acting from the left) and ${}_{(n)}(\leftarrow)$, ${}_{(n)}(\rightarrow)$ (acting from the right), which for the example of Fig. 3 read

$$ {}_{(5)}(\downarrow)=\begin{bmatrix}0&0&0&0&1\\1&0&0&0&0\\0&1&0&0&0\\0&0&1&0&0\\0&0&0&1&0\end{bmatrix}={}_{(5)}(\leftarrow) \tag{15}$$

and correspondingly, by inversion, in the other cycling directions. In general, however, Eq. (13) expresses that opposite directions are quantum mechanically superposed with equal weights, and it is notationally convenient then to introduce the ν'th floor "quantum paternoster" operator symbol

$$ {}_{(n)}(\uparrow\downarrow)_{\nu'}\equiv\frac{{}_{(n)}(\uparrow)^{\nu'}+{}_{(n)}(\downarrow)^{\nu'}}{2} \tag{16}$$

for row and, by analogy, ${}_{n}(\leftrightarrows)_{\mu'}$ for column rotations. It is then possible to write Eq. (13) in matrix form, i.e.,

$$ {}_{(n)}\Psi\left(2\pi\frac{m}{n}\right)=\left[\sum_{\nu'=1}^{n}C(\nu',Mm,n)_{(n)}(\uparrow\downarrow)_{\nu'}\right]{}_{(n)}\Psi(0)\times\left[\sum_{\mu'=1}^{n}C(\mu',Nm,n)_{(n)}(\leftrightarrows)_{\mu'}\right]. \tag{17}$$

The beauty of this formulation is that the billiard table (square, due to the chosen rationalization) can be directly identified with a square matrix, which leads to an inherently pictorial way of looking at the problem. This, in an unusual way, is "matrix mechanics" in its purest form. The requirement that a time skip mT/n can be equivalently thought of as a composition of m elementary time steps T/n finds a particularly simple expression within this formalism. It implies that expression (17) is equivalent to

$$ {}_{(n)}\Psi\left(2\pi\frac{m}{n}\right)=\left[\sum_{\nu'=1}^{n}C(\nu',M,n)_{(n)}(\uparrow\downarrow)_{\nu'}\right]^{m}{}_{(n)}\Psi(0)\times\left[\sum_{\mu'=1}^{n}C(\mu',N,n)_{(n)}(\leftrightarrows)_{\mu'}\right]^{m}. \tag{18}$$

At this point there is no need anymore to depict the whole 2π periods along ξ and η in our graphics. Figure 4, for instance, shows merely the billiard plane itself (notice the axes labels) and the evolution of an "F" initially placed into one of its corners after a time $T/4$. The resulting matrix expressions are shown for three different aspect ratios. Since the coefficients $C(1,2,4)$, $C(3,2,4)$, $C(4,2,4)$, $C(1,3,4)$, and $C(3,3,4)$ all vanish, no other possibilities than those of the figure exist. [That is, once more excluding the trivial exact revivals that are obtained if the fraction M/N is reducible.] The remaining coefficients in this case read $C(2,2,4)=1$, $C(2,3,4)=(1-i)/2$, and $C(4,3,4)=(1+i)/2$.

So far, in our graphics we have used wave distributions shaped similar to an "F" in order to show unambiguously how the images become periodically rotated and mirrored inside a billiard. Now that this behavior has become clear, however, we will only consider "blobs" of matter that are symmetric both along the x (ξ) and along the y (η) axis. By doing so, the shape of the blob, being merely a common factor, can be pulled out of the matrices, as depicted symbolically in Fig. 5. The actual shape of the blob becomes irrelevant and the remaining, square matrices just contain complex numbers which we will assume to be normalized in such a way, that the sum of their squared moduli equals 1. By stroboscopically synchronizing the detection of trapped atoms with the—intrinsically periodic—emergence of fractional revivals in a given billiard, a set of blobs of identical

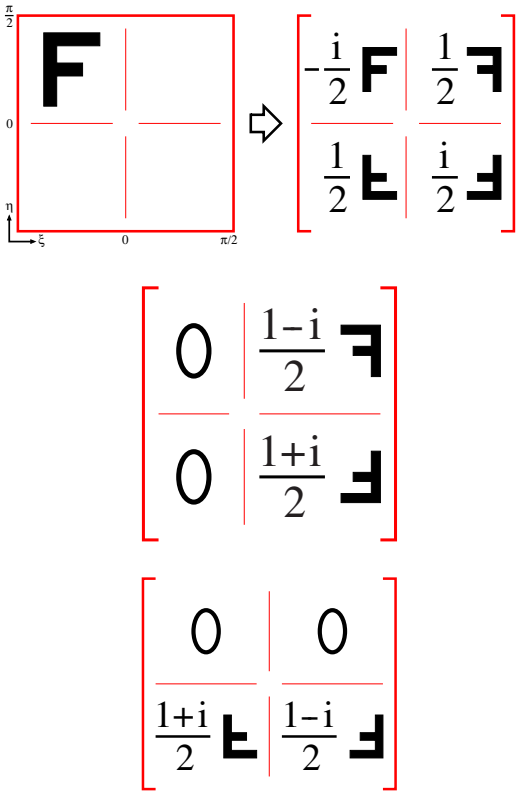

FIG. 4. (Color online) The insight gained by the tiling introduced in Fig. 3 allows us, first, to concentrate fully on the proper billiard itself, as shown on the left-hand side of (a). As shown in the same part (a) on the right-hand side, it allows us, second, to equivalently substitute the (square) billiard plane by a (square) matrix. The cross drawn with thin lines has only been introduced as a guide for the eye. If a wave amplitude in the shape of an "F" is initially placed into one corner of the billiard, as shown on the left of (a), its time development will again depend on the aspect ratio of the considered billiard (i.e., before its rationalization). Three cases are illustrated for the same instant of time, $\tau=\pi/2$. The right side of (a) applies to the case $M=1$, $N=1$. The situation for $M=1$, $N=2$ is depicted in (b). Finally, (c) illustrates what happens if $M=2$, $N=3$.

shape but varying amplitudes and phases (and conserved total intensity, i.e., norm) will be observed. Such intermittent and nondestructive detection methods, based for instance on far off-resonance phase imaging techniques, are common-

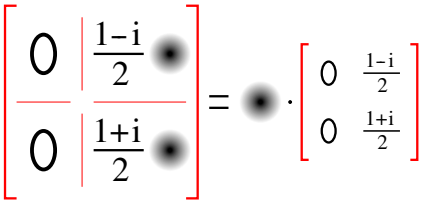

FIG. 5. (Color online) We define a "blob" as a billiard-internal wave function which is symmetric both along the ξ and η directions. At periodically timed space intervals, it becomes possible to "pull" these blobs out of the matrices, which then end up containing but numeric values, as illustrated in this figure. The situation depicted corresponds to the case shown in Fig. 4(b).

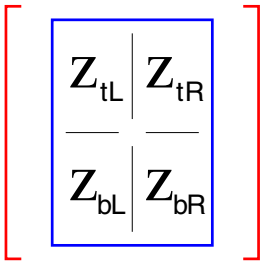

FIG. 6. (Color online) The figure makes explicitly clear, how the orientation of the A4 billiard introduced in the main text is defined. It also shows how the corresponding matrix elements are called and what the short forms "tL" (top left), "bL" (bottom left), "tR" (top right), and "bR" (bottom right) actually stand for.

place in time-domain atom optics experiments in order to minimize the influence of the measuring apparatus on the system that is being observed. The fact that real-life billiard walls are of course neither perfectly hard nor infinitely high leads to a loss of revival fidelity, caused especially by the higher modes, which are by nature more susceptible to the detailed shape of the optical potential that defines a billiard cushion. Blobs with a soft, approximately Gaussian intensity profile are therefore particularly convenient in the sense that, on the one hand, their power spectrum falls off rather quickly and, on the other, they are generally quite easy to produce.

IV. THE "A4" ($M=1$, $N=2$) BILLIARD

Deviations from ideal wall characteristics set a *lower* limit to the physical size that a billiard can attain before it loses its fractional revival qualities. Since, according to Eq. (8), the revival time in a two-dimensional billiard is proportional to the enclosed area, an *upper* limit to its physical size is defined by the average trap lifetime (to which various different loss mechanisms usually contribute and which can nowadays be as large as a few seconds and even more). For a given billiard area, the aspect ratio parameters M and N should be chosen to be as small as possible. The simplest and possibly most convenient choice turns out to be $M=1$ and $N=2$, which corresponds to a billiard in the shape of an A4 paper sheet.

A. Vectorial representation and transformation matrices

For our intended purposes, we choose a revival time division factor of $n=4$, which (compare with Fig. 3) requires us to divide the billiard into four symmetric sectors, as shown in Fig. 6. Sectors will be labeled as indicated in the figure and one blob will be placed in each of them. The amplitude and phase of each blob will be interpreted as the information content of its sector, which then plays the role of a register. We will treat these registers on an equal footing and thus prefer to write them using a column vector notation of the form

$$\begin{bmatrix} z_{tR} \\ z_{tL} \\ z_{bR} \\ z_{bL} \end{bmatrix}. \tag{19}$$

For convenience, whenever from now on we talk about the "right" and "left" (or, alternatively, about the "top" and "bottom") sections of the trap, we will be explicitly referring to the rectangle orientation depicted in Fig. 6.

The discretized time evolution inside the billiard is described by a set of unitary matrices acting on the vector (19). We will denote the matrix corresponding to a time step of m/n by $R_{m/n}$. For instance, the situation depicted in Fig. 2(b) (assuming a symmetric distribution) is mathematically expressed by the matrix

$$R_{1/2} = -\begin{bmatrix} 0 & 0 & 1 & 0 \\ 0 & 0 & 0 & 1 \\ 1 & 0 & 0 & 0 \\ 0 & 1 & 0 & 0 \end{bmatrix}. \tag{20}$$

Similarly, the situation of Fig. 4(b) is described by

$$R_{1/4} = \frac{e^{i\pi/4}}{\sqrt{2}}\begin{bmatrix} 0 & i & 0 & 1 \\ i & 0 & 1 & 0 \\ 0 & 1 & 0 & i \\ 1 & 0 & i & 0 \end{bmatrix}. \tag{21}$$

One readily verifies that $R_{1/4}^2 = R_{1/2}$ and that $R_{1/2}^2 = 1$, as it should be. Quite unexpectedly, however, the numerical simulation of a billiard with these proportions shows that blobs are reconstructed *also* at 1/8, 3/8, 5/8, etc. of the revival time. In order to analytically see the reason for this, one needs the following coefficients: $C(1,1,8) = C(3,1,8) = C(5,1,8) = C(7,1,8) = C(1,2,8) = C(2,2,8) = C(3,2,8) = C(5,2,8) = C(6,2,8) = C(7,2,8) = 0$, $C(2,1,8) = C(6,1,8) = 1/2$, $C(4,1,8) = (e^{i3\pi/4})/2 = -C(8,1,8)$, $C(4,2,8) = (e^{i\pi/4})/\sqrt{2} = C(8,2,8)^*$. A straightforward calculation then demonstrates that the wave function at $m/n = 1/8$ consists of a weighted superposition of the four possible mirror images of the initial wave function (taking Fig. 1 as an example, all symmetry variations of "F" become coherently combined). Since here we are considering blobs that are by definition symmetric along both Cartesian axes, the blob image can once more be pulled out of the matrix, which then reads

$$R_{1/8} = \frac{e^{-i7\pi/8}}{\sqrt{8}}\begin{bmatrix} \sqrt{2-\sqrt{2}} & -i\sqrt{2-\sqrt{2}} & i\sqrt{2+\sqrt{2}} & \sqrt{2+\sqrt{2}} \\ -i\sqrt{2-\sqrt{2}} & \sqrt{2-\sqrt{2}} & \sqrt{2+\sqrt{2}} & i\sqrt{2+\sqrt{2}} \\ i\sqrt{2+\sqrt{2}} & \sqrt{2+\sqrt{2}} & \sqrt{2-\sqrt{2}} & -i\sqrt{2-\sqrt{2}} \\ \sqrt{2+\sqrt{2}} & i\sqrt{2+\sqrt{2}} & -i\sqrt{2-\sqrt{2}} & \sqrt{2-\sqrt{2}} \end{bmatrix}. \tag{22}$$

This elementary time step, e.g., one eighth of the full revival period, we shall define as our fundamental *clock cycle*. The natural clock frequency of the A4 billiard is therefore twice as large as naïvely expected. As demonstrated numerically in Ref. [8], the time windows at the blob revival times are rather large and easily allow one to impinge controlled phase shifts ϕ_{ij} on each blob by means of suitable laser pulses (i.e., via the dynamic Stark shift),

$$P_{\phi_{tR},\phi_{tL},\phi_{bR},\phi_{bL}} \equiv \begin{bmatrix} e^{i\phi_{tR}} & 0 & 0 & 0 \\ 0 & e^{i\phi_{tL}} & 0 & 0 \\ 0 & 0 & e^{i\phi_{bR}} & 0 \\ 0 & 0 & 0 & e^{i\phi_{bL}} \end{bmatrix}. \tag{23}$$

As we will show next, with the help of the ingredients (22) and (23) it becomes possible to manipulate the four registers z_{tR}, z_{tL}, z_{bR}, z_{bL} at will.

B. Generation of arbitrary states

In order to demonstrate how this works, let us assume that a single blob has been deposited in the upper right billiard register, so that initially the system's state is described by

$$\begin{bmatrix} 1 \\ 0 \\ 0 \\ 0 \end{bmatrix}. \tag{24}$$

Our goal is to show that this state can be transformed into any arbitrary state of our choice. The transformation (20) is little useful for this purpose, inasmuch as it merely interchanges the upper and lower halves of the billiard. The possibilities offered by $R_{1/4}$ are richer and have already been discussed in Ref. [8]. There it was noticed that

$$P_{0,-3\pi/4,0,-\pi/4} R_{1/4} \begin{bmatrix} 1 \\ 0 \\ 0 \\ 0 \end{bmatrix} = \frac{1}{\sqrt{2}}\begin{bmatrix} 0 \\ 1 \\ 0 \\ 1 \end{bmatrix}. \tag{25}$$

By introducing a relative phase shift α between the two components, an arbitrary splitting ratio $|z_{tR}|/|z_{bR}|$ can be obtained after a further $R_{1/4}$ operation,

$$R_{1/4}\frac{1}{\sqrt{2}}\begin{bmatrix}0\\ e^{i\alpha}\\ 0\\ 1\end{bmatrix}=\frac{i}{2}\begin{bmatrix}e^{i(\alpha+\pi/4)}+e^{-i\pi/4}\\ 0\\ e^{i(\alpha-\pi/4)}+e^{i\pi/4}\\ 0\end{bmatrix}=\begin{bmatrix}z_{tR}\\ z_{tL}\\ z_{bR}\\ z_{bL}\end{bmatrix}, \quad (26)$$

for

$$|z_{tR}|^2=\frac{1-\sin\alpha}{2} \quad (27)$$

and

$$|z_{bR}|^2=\frac{1+\sin\alpha}{2}. \quad (28)$$

On the other hand, the $R_{1/4}$ operator is incapable of changing an initially given splitting ratio between the left and the right side's total intensities. That means that, irrespective of the chosen input state, the identity

$$R_{1/4}\begin{bmatrix}z'_{tR}\\ z'_{tL}\\ z'_{bR}\\ z'_{bL}\end{bmatrix}=\begin{bmatrix}z_{tR}\\ z_{tL}\\ z_{bR}\\ z_{bL}\end{bmatrix} \quad (29)$$

satisfies $|z'_{tR}|^2+|z'_{bR}|^2=|z_{tL}|^2+|z_{bL}|^2$ and $|z'_{tL}|^2+|z'_{bL}|^2=|z_{tR}|^2+|z_{bR}|^2$. Consecutive applications of $R_{1/4}$ will thus only swap the summed intensities between the left and the right half of the billiard, yet without ever being able to modify them. It can be considered quite fortunate (in the sense of not being *a priori* obvious), that $R_{1/8}$ allows to do precisely this, thus leading to a simple and intuitive algorithm for the preparation of arbitrary quantum states. In order to see how this works, we first notice that in the same time that it takes to symmetrically split the initial blob (24) into a top-and-bottom superposition state according to Eq. (25), it is equally possible to create a symmetric left-and-right superposition by applying the operator series

$$R_{1/8}P_{0,\pi/2,\pi,3\pi/2}R_{1/8}\begin{bmatrix}1\\ 0\\ 0\\ 0\end{bmatrix}=\frac{1}{\sqrt{2}}\begin{bmatrix}1\\ 1\\ 0\\ 0\end{bmatrix}. \quad (30)$$

By introducing a relative phase β between the two resulting components, an arbitrary splitting ratio $(|z_{tR}|^2+|z_{bR}|^2)/(|z_{tL}|^2+|z_{bL}|^2)$ can be obtained after a further $R_{1/8}$ operation,

$$R_{1/8}\frac{1}{\sqrt{2}}\begin{bmatrix}e^{i\beta}\\ 1\\ 0\\ 0\end{bmatrix}=\begin{bmatrix}z_{tR}\\ z_{tL}\\ z_{bR}\\ z_{bL}\end{bmatrix}, \quad (31)$$

for

$$|z_{tL}|^2+|z_{bL}|^2=\frac{1+\sin\beta}{2} \quad (32)$$

and

$$|z_{tR}|^2+|z_{bR}|^2=\frac{1-\sin\beta}{2}. \quad (33)$$

With this insight, we have in our hands a simple recipe for creating an arbitrary state with components d_{tR}, d_{tL}, d_{bR}, and d_{bL} out of Eq. (24). First of all, one creates the superposition state defined in Eq. (30). Next, one evaluates the value of $|d_{tL}|^2+|d_{bL}|^2$ and determines β from Eq. (32). A phase of this size should then be impinged on the upper right blob. After waiting for one clock cycle, the correct relative populations between the left and the right sectors of the billiard will have been established. The correct ratios between $|d_{tR}|$ and $|d_{bR}|$, on the right side, and $|d_{tL}|$ and $|d_{bL}|$ on the left side of the billiard can be now adjusted by inducing appropriate phase shifts α_R and α_L on each side, and letting pass 1/4th of the revival time. At this stage, the magnitudes $|d_{tR}|$, $|d_{tL}|$, $|d_{bR}|$, and $|d_{bL}|$ will have been correctly distributed in the billiard plane. The only thing that remains to be done is to correct the phases as required. All in all, the described process takes up five elementary clock cycles. This does not of course imply that particular states cannot be produced faster. However, it does demonstrate that it is possible to develop an intuitive feeling for the dynamics and to use this understanding to achieve intended goals in a systematic way. Numeric tools may be used instead to determine the *optimum* procedure to be employed for a given task. Although at this stage we are more interested in providing but a proof of principle, optimization aspects would definitely become important in the moment of practical implementation.

C. Quantum search in a billiard

Our following example has been chosen to illustrate these ideas. It demonstrates how Grover's paradigmatic "quantum search algorithm" [33] could be realized in a billiard system. This algorithm was conceived to transform the initially unobservable phase marking of a single item in a quantum list (e.g., in our present case, one of the entries in a four-dimensional column vector) into an easily identifiable amplitude marking.

We begin with an "unbiased" state, i.e., one of the form

$$\frac{1}{2}\begin{bmatrix}1\\ 1\\ 1\\ 1\end{bmatrix}. \quad (34)$$

It can be quite intuitively constructed by starting with an initial, single blob (placed, for instance, in the upper right billiard corner) and splitting it once along the top-bottom axis and once along the perpendicular, left-right axis of the billiard. A final phase correction leads to the desired state, i.e.,

$$e^{-i\pi/4}P_{-\pi/2,-\pi/2,0,0}R_{1/4}R_{1/8}P_{0,\pi/2,\pi,3\pi/2}R_{1/8}\begin{bmatrix}1\\0\\0\\0\end{bmatrix}=\frac{1}{2}\begin{bmatrix}1\\1\\1\\1\end{bmatrix}. \tag{35}$$

Here we have used the fact that the matrix representation of the triple operator product in the splitting sequence of Eq. (30) is block diagonal,

$$R_{1/8}P_{0,\pi/2,\pi,3\pi/2}R_{1/8}=\frac{1}{\sqrt{2}}\begin{bmatrix}1&1&0&0\\1&-1&0&0\\0&0&-1&-1\\0&0&-1&1\end{bmatrix}. \tag{36}$$

Standard imaging techniques are sensitive to amplitudes only. Detectors of this sort will not be able to discern the four states

$$\frac{1}{2}\begin{bmatrix}-1\\1\\1\\1\end{bmatrix},\quad \frac{1}{2}\begin{bmatrix}1\\-1\\1\\1\end{bmatrix},\quad \frac{1}{2}\begin{bmatrix}1\\1\\-1\\1\end{bmatrix},\quad \frac{1}{2}\begin{bmatrix}1\\1\\1\\-1\end{bmatrix} \tag{37}$$

obtained by impinging a π phase on one and only one of the components of our unbiased state (34). Grover's algorithm allows one to transform these phase-marked states into corresponding amplitude-marked ones. It does so in such a way that a one-to-one correspondence is established, thus allowing to unambiguously identify each of the states (37).

A billiard version of this algorithm can be constructed by slightly generalizing Eq. (35). In a first step, we identify an operational means to bijectively transform the state of a single initial blob placed in any one of the four billiard quarters into each of the phase-marked states (37). The fact that the blob starting position is *a priori* unknown implies that some of the required phase-shifting pulses will actually hit empty space. These "shots in the dark" are indeed a basic and intuitively expected feature of such an algorithm. The following time series demonstrates how it goes:

$$P_{0,-\pi/2,-\pi/2,0}R_{1/4}P_{-\pi/2,0,0,\pi/2,}R_{1/8}P_{0,\pi/2,\pi,3\pi/2}R_{1/8}P_{\pi/4,\pi/4,\pi/4,-3\pi/4}\begin{bmatrix}1&0&0&0\\0&1&0&0\\0&0&1&0\\0&0&0&1\end{bmatrix}=\frac{1}{2}\begin{bmatrix}-1&1&1&1\\1&1&-1&1\\1&-1&1&1\\1&1&1&-1\end{bmatrix}. \tag{38}$$

In a second step, we now invert this operator sequence. To do so, it is convenient to make use of the time-reversal relations

$$R_{1/4}^{-1}=e^{i\pi/2}P_{\pi,\pi,0,0}R_{1/4}P_{\pi,\pi,0,0} \tag{39}$$

and

$$R_{1/8}^{-1}=e^{-i\pi/4}P_{\pi,0,0,\pi}R_{1/8}P_{\pi,0,0,\pi}. \tag{40}$$

With their help, we finally obtain

$$e^{i3\pi/4}P_{\pi,0,0,0}R_{1/8}P_{3\pi/2,\pi,\pi/2,0}R_{1/8}P_{0,\pi/2,-\pi/2,0}R_{1/4}P_{\pi,3\pi/2,\pi/2,0}\frac{1}{2}\begin{bmatrix}-1&1&1&1\\1&1&-1&1\\1&-1&1&1\\1&1&1&-1\end{bmatrix}=\begin{bmatrix}1&0&0&0\\0&1&0&0\\0&0&1&0\\0&0&0&1\end{bmatrix}. \tag{41}$$

D. Scalability—classical vs quantum computers

By appropriately introducing a new wall at the geometric center of an A4 billiard, two billiards of the same aspect ratio as the original one are obtained. This of course is the spirit of the International Organization for Standardization (ISO) 216 norm that conveniently defines paper sheet aspect ratios by an iterative process of symmetric dichotomies (leading to the standard series denominated A0, A1, A2, A3, A4, etc.). This is important to notice, since it easily allows us to extend our previous results involving the four registers of a single billiard to a cascade of nested, self-similar "billiard onions," thus providing a proportionally larger number of sectors, as represented symbolically in Fig. 7.

There exist at least two good reasons to be interested in the scalability of these kinds of systems. It had indeed already been proposed in Ref. [8] to interpret billiards as time-domain interferometric devices. In this sense, billiard-in-a-billiard architectures enable one to generalize the analog of an elementary two-arm Mach-Zehnder interferometer to multiple-path interference machines. Also for these larger compounds it remains true that any conceivable state can be generated. This crucial insight we would also like to illus-

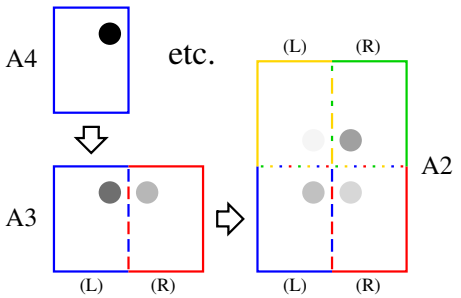

FIG. 7. (Color online) By removing the wall between two adjacent $M=1$, $N=2$ billiards, a new billiard with the same aspect ratio is obtained. If the possibility to individually turn the intermediate walls (dashed, dotted, and dash-dotted in this figure) on or off is contemplated, it becomes possible to create "nested" billiard architectures. The blobs illustrate the method described in the main text to create arbitrary states in such systems.

trate with the help of Fig. 7 and the nomenclature defined therein.

The large A2 billiard on the right-hand side of the figure comprises four elementary A4 traps with four registers each, thus spanning a sixteen dimensional complex vector space. Given an arbitrary (normalized) vector that we want to construct, three steps are required for this purpose. First of all we must make sure that every A4 sector in the A2 billiard contains the correct intensity. Once this has been achieved, the internal walls separating the four sections should be turned on and each separate A4 billiard be manipulated according to the recipe given in Sec. IV B in order to produce the desired pattern. Finally, the internal walls can be removed again and the target state will be ready. Steps 2 and 3 do not involve anything new, so that only step 1 needs to be considered in more detail. As will be made clear in the next paragraph, this first step does *not* require operation $R_{1/8}$ at all. Consequently, there is no need whatsoever to presuppose wave functions of a particular symmetry, as we had already made visually clear in Figs. 2(b) and 4(b).

Here is how it goes. Starting point, as in Sec. IV B, is a single blob in an A4 billiard, compare Fig. 7. Next, one determines the desired total intensity on the left (L) and right (R) sides of billiard A2 from the rated values of the final state to be constructed. In order to correctly produce this intensity ratio, the right border of A4 (i.e., the dashed line in the billiard A3) must be removed and steps (25) and (26) be applied to the resulting billiard (A3, see Fig. 7). This leads to a pair of (generally nonidentical) blobs, as symbolically depicted. Now that the (L) and (R) intensities are correctly implemented, the desired up and/or down intensity ratios on each side can be calculated, all the internal walls in A2 be removed and steps (25) and (26) be applied to this larger (A2) billiard. At this stage, A2 will contain one blob of the correct intensity in each of its four sectors and our goal will have been met.

1. Classical computers

Now that it has become clear that arbitrary states can be created in such a nested system of billiards, it has at the same time been shown that the states can be manipulated at will. Since the probability densities in each "register" can also be nondestructively measured by phase-imaging techniques, information feedback mechanisms become feasible. These billiard systems can therefore be viewed as (classical) analog computers in which the external, continuous control knobs are represented by the phases that can be independently induced in each billiard sector. In the atom optics context, this corresponds to interpreting these two-dimensional trap arrays as "atom chips" that (stroboscopically) operate in the time domain and which, according to what has already been demonstrated, can in principle be made as complex as desired.

The advantage of a time-domain approach to atom chips can be illustrated by the fact that the first manifestly *coherent* atom beam splitter on such devices was demonstrated in this manner [34], years after the introduction of an analogous component that operated in the spatial domain [35]. Such an element is of course a basic building block for the construction of atom interferometers. One drawback of the rf-field approach described in Ref. [34] (or in the earlier magnetic microtrap proposal of Ref. [36]) is that care must be taken to change the involved atom-optical potentials slowly enough as to guarantee the adiabaticity of the wave function splitting process in all moments. On the contrary, our proposed time-domain "beam" splitter, as described for instance by Eqs. (25) and (30), does not involve any "moving parts" in the sense of those adiabatically varying, external potentials. It is intrinsically coherent and the time it takes to spatially separate a wave packet depends exclusively on the built-in time scale, i.e., the revival period (8) of the chosen system.

This leads us directly to the second reason, why the scalability issue could be of utmost importance, namely in view of the possibility to use these extended billiard systems as a platform for (decoherence-time limited) quantum information processing.

2. Quantum computers

It is conceptually important to keep emphasizing that the mere fact that we are talking about matter waves does not imply that the billiard systems under scrutiny are themselves quantum computers. The phenomena discussed so far could be well reproduced in an entirely classical frame using, for instance, electromagnetic waves [4] or perhaps even water waves.

Instead, the idea is to store the quantum information that one intends to process in the *internal* state of the atoms trapped in the billiard and to use the billiard as a means to manipulate the *external*, i.e., motional atomic degree of freedom.

Most typically, qubits in atom optics are physically represented by suitably chosen two-level atomic transitions. Different proposals to implement universal quantum gates with neutral atoms have been put forward [33]. Essential in all these schemes is that two trapped atoms can be brought together and later separated again in a controlled way. In the methods proposed so far, the required (adiabatic) particle motion can be visualized and interpreted in classical terms.

Wave billiards, on the contrary, can be used to achieve the same goal in a more subtle, manifestly quantum-mechanical fashion. If we again consider an elementary (i.e., not nested)

A4 trap as an example, we notice that the operator $R_{1/8}$ is not required for the mere purpose of moving atom blobs around. If we thus do not make use of single $2\pi/8$ time steps, this implies, as we have already seen, that the left- and the right-hand sides of the billiard do not become mingled if observed at the corresponding fractional revival times. Thus, instead of dealing with a four-dimensional complex vector space, one would be effectively facing a physical situation representable by a pair of mutually independent, two-dimensional complex vector spaces.

Without loss of generality, we may therefore assume that precisely two atoms are initially loaded into such a billiard, say, into the top and bottom registers on its left-hand side. Since their wave function will become delocalized, forming a pair of distinct blobs on the right-hand side of the billiard after $1/4$ of a revival cycle, it is the dynamics of a billiard itself that periodically—and without further ado—brings the atoms spatially together in such a scheme. The implementation of a fast ("Rydberg") phase gate based on an externally triggered electric-dipole interaction [37] appears particularly promising in this context. (The magnetic-dipole quantum gate proposed in Ref. [38], on the other hand, would be problematic, inasmuch as the phase-inducing interaction is then necessarily "always on.")

3. Conveyor belts

Despite its experimental difficulty, the deterministic delivery of single atoms into traps made of light has already been repeatedly demonstrated. An interesting example involves the controlled loading of an optical conveyor belt with a preestablished number of atoms [39,40]. Figure 8 shows two possible ways to realize optical conveyor belts by alternatingly switching between a linear series of overlapping billiards. As in Ref. [40], one expects such a device to be coherence preserving. Scheme 8(b) is faster than 8(a) by a factor of $\sqrt{2}$. Of course, both devices should in principle work perfectly well even if they are loaded with clouds of atoms, which is actually the more common situation encountered in ("macroscopic") atom optics. If the particles are in the Bose-condensed state, however, nonlinear effects produced by weak atomic interactions can lead to a highly nontrivial time evolution [41]. Fundamental limits for integrated atom optics with Bose-Einstein condensates have been identified [42]. It is still an open question, if nonlinearities in quantum billiard systems can be employed to create useful nonlinear atom optical components.

V. CONCLUSIONS

We have developed a convenient formulation of the fractional dynamics that governs the time development in a well-defined class of quantum billiards. In the two-dimensional case, we extensively discuss the important example of rectangular billiards with aspect ratios that are known to lead to regular dynamic behavior. The simplicity of our treatment should allow its inclusion in elementary quantum mechanics lectures. Particle identity aspects could also be easily taken into account in a pedagogical context.

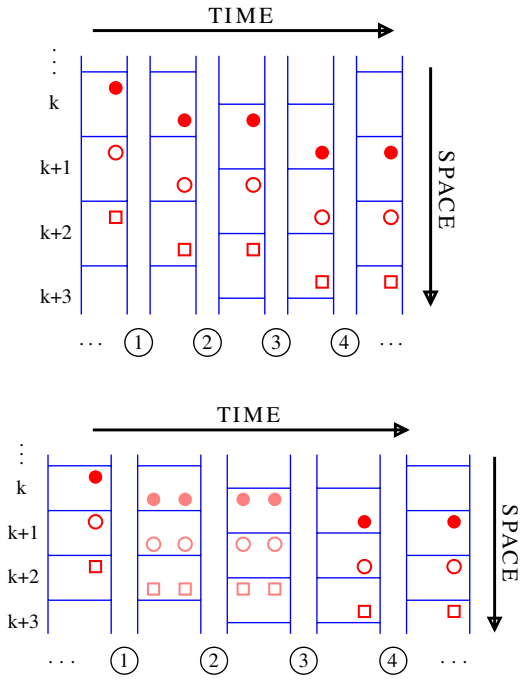

FIG. 8. (Color online) A ribbon made of consecutive adjacent billiards can be used to spatially transport blobs as in a "bucket brigade," if one allows for the possibility to switch between alternating billiard walls, as illustrated in the two schemes of (a) and (b). In order to perceive the motion of the various blobs more clearly, they have been coded with different shapes.

Billiards with proportions identical to an A4 paper sheet have the important and distinct advantage that the introduction of just one additional wall can split the initial rectangle into a pair of geometrically similar ones. This property is not shared by the sole more elementary and particularly symmetric paradigm of a rectangular billiard, i.e., the square one. For this reason, we decided to pay special attention to the possibilities offered by these A4 systems. This finally led us to consider billiard-in-a-billiard architectures.

By stroboscopically restricting the observation of quantum wave evolution to appropriately defined time intervals, the arising revival structures offer a possibility of interpreting the billiard plane as a collection of information-carrying registers. Their time development can be expressed in terms of discrete (unitary) matrix transformations. We present a constructive method for generating arbitrary states in the so-defined Hilbert space. For this purpose, the only requirement is the ability to modify the phases of the individual registers at will.

This leads to a direct link to interferometry, since it allows to transform invisible phase differences into easily detectable intensity signals. As a tangible example, we demonstrate how the billiard-version of Grover's (quantum) search algorithm could be implemented. Nested billiard systems generalize these concepts and lead to the analog of multiple path interferometric devices.

The possibility to experimentally realize these ideas is illustrated with the example of atom optics. Revival times are inversely proportional to the mass of the trapped particle. Their minimization is crucial for the construction of

coherence-time limited devices, such as quantum computers. Also electrons in semiconducting billiards [43] could be used to implement the proposals discussed in this paper.

As far as the fractional wave evolution itself is concerned, probably the simplest way of illustrating the rich dynamic behavior would make use of electromagnetic waves. By exploiting the mathematical analogy to situations encountered in the optics context (and briefly analyzed in the Appendix A), a waveguide with rectangular cross section would, for instance, serve this purpose. Another—maybe more immediate and pictorial—possibility is to employ correspondingly shaped microwave billiards [44].

Now that a comfortable framework for the description of the dynamics inside of "rational" rectangle billiards has been established, it would be interesting to extend our understanding by including additional variables. Ideally, these should involve currently available experimental possibilities. With the invention of laser "scanning" atom traps [45], for instance, it has become feasible to study resonant phenomena in rotating rectangular billiards [46]. New opportunities are opened by our current ability to load atom chips with degenerate, weakly interacting fermions [47]. In a recent experiment involving graphene, the phase-coherent transport of fermions in quantum billiards has been investigated in a completely different kind of systems [48]. In view of these developments, we expect our study to represent a convenient starting point for the analysis of more complex and physically richer billiard models.

ACKNOWLEDGMENTS

I would like to express my deep and sincere gratitude to Professor B.-G. Englert for the hospitality experienced during my visit of the QIT-Lab at the National University of Singapore. This work was partially supported by an A*STAR Temasek Grant No. 012-1014-0040 (Singapore).

APPENDIX A: TALBOT EFFECT

Quantum billiard revivals are closely related to an optical self-imaging phenomenon known as the Talbot effect [49]. Here we briefly elucidate this connection. Let us consider the case of a plane monochromatic wave propagating along the positive z direction,

$$\psi(x,z<0,t)=e^{-i\omega t}e^{ik_z z}. \tag{A1}$$

At $z=0$, it traverses a (strictly periodic) grating of transmittance

$$T(x)=\sum_{\mu=-\infty}^{\infty}T_\mu e^{i\mu k_x x}, \tag{A2}$$

for which two assumptions are made. First, the grating constant should be much larger than the employed wavelength, $k_x \ll k_z$. Second, beyond the evanescent cutoff diffraction order $\bar{\mu}\equiv k_z/k_x$, the Fourier expansion contribution shall be negligible, $\Sigma_{|\mu|>\bar{\mu}}|T_\mu|^2 \ll 1$. Under these circumstances, the paraxial approximation can be applied and leads to a propagation kernel of the Fresnel-Kirchhoff type [50],

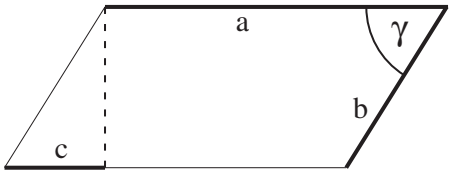

FIG. 9. Definition of angle γ and segments a, b, and c in a parallelogram, as used in Appendix A.

$$\psi(x,z\geq 0,t)=e^{-i\omega t}e^{ik_z z}\sqrt{\frac{k_z}{i2\pi z}}\int_{-\infty}^{\infty}dx' T(x')e^{ik_z(x-x')^2/(2z)}. \tag{A3}$$

It essentially modulates the incoming wave (A1) by a manifestly x-periodic and not-so-evidently z-periodic factor, as can be explicitly verified by introducing series (A2) into Eq. (A3), thus obtaining

$$\psi(x,z\geq 0,t)=e^{-i\omega t}e^{ik_z z}\underbrace{\sum_{\mu=-\infty}^{\infty}T_\mu e^{i\mu k_x x}e^{-i2\pi\mu^2 z/Z}}_{=T(x)\ \text{at}\ z=0,Z,2Z,3Z,\ldots}. \tag{A4}$$

Here $Z\equiv 4\pi k_z/k_x^2$ denotes the self-imaging or "Talbot" revival distance. This result slightly generalizes expression (2) inasmuch as $T(x)$ is not required to periodically vanish as in the billiard case. (A completely analogous—optical—situation in which the function is assumed to equal zero on the boundaries arises in coherent waveguide image transmission. See Ref. [9] for a thorough mathematical treatment and Ref. [51] for a review.) Fractional revivals (or "Fresnel images") are again obtained by introducing (Talbot) coefficients $C(\mu',m,n)$ and making use of their defining properties, Eqs. (3) and (4). Although these results are *monnaie courante* in the optics community, this is generally untrue for other areas of research, and quantum mechanics in particular [52]. In view of the school-level simplicity of the solution (and its resulting mathematical wealth and beauty [53]), this is quite astonishing and one is spontaneously led to ask, paraphrasing Gori, why the Fresnel transformation is so little known [54].

In the two-dimensional case, there exist a larger set of diffracting structures capable of self-imaging [55]. Doubly periodic gratings, in particular, produce Talbot images if and only if the squared ratio, $(a_x/a_y)^2$, of their periods along the orthogonal directions x and y is a rational number. Since the wave function is not required to vanish on the unit cell borders, there are no restrictions concerning their geometric shape. This makes the situation quite more general than in the case of billiards, where tiling requirements have been shown to be extremely stringent. (Although rectangular unit cells lead to the simplest formulation of the self-imaging criterion, other possibilities have been considered in the literature as well [56]. Tiling with parallelograms characterized by their side lengths a, b, and the enclosed angle γ—see Fig. 9—has for instance been studied in Ref. [57]. Indeed, the resulting pair of conditions, e.g., the quantities $(a/b)\cos\gamma$ and $(a/b)^2$ to be both rational, immediately lead to the re-

quirement c/a to be a rational number as well. This implies that the two-dimensional grating in fact possesses rectangular unit cells and that their side-length ratio leads to Talbot revivals. Hexagonal rasters satisfy the self-imaging criterion, too. They play a role in insect vision [58,59] and they may turn out to be useful in the context of atom optics nanofabrication as well [60,61].)

APPENDIX B: LANDSBERG-SCHAAR FORMULA

There exist many useful relations among the coefficients $C(\mu',m,n)$. Most of them are quite easy to prove, such as Eq. (14). Here we derive one of the less trivial examples. It is related to the so called "Landsberg-Schaar formula" for quadratic Gauss sums, which plays a key role in analytic number theory and states that for any positive integers m and n

$$\frac{e^{-i\pi/4}}{\sqrt{2m}}\sum_{j=1}^{2m}\exp\left(i2\pi\frac{nj^2}{4m}\right)=\frac{1}{\sqrt{n}}\sum_{j=1}^{n}\exp\left(-i2\pi\frac{mj^2}{n}\right). \tag{B1}$$

The standard proof of this identity (as given, for instance, in Ref. [62]) presupposes detailed knowledge of theta functions and their behavior around singular points. A physically inspired, yet rigorous proof of Eq. (B1) that avoids the need for higher functions and nontrivial limiting processes was recently described in [63].

Here we present a short and straightforward "physicist's derivation" of expression (B1). It is not intended to be a strict mathematical proof in the above sense. But rather tries to capture the essence of the problem by interpreting it in terms of the introductory textbook example of diffraction at a grating made of infinitely narrow slits. Starting with Eq. (A3) and rationalizing units by defining $\xi\equiv k_x x$ and $\zeta\equiv 2\pi z/Z$, propagation within the paraxial approximation is described by

$$\psi(\xi,\zeta>0)=\frac{1}{\sqrt{i\pi 4\zeta}}\int_{-\infty}^{\infty}d\xi'\exp\left[i\frac{(\xi'-\xi)^2}{4\zeta}\right]\psi(\xi',0). \tag{B2}$$

Here, $\psi(\xi',0)$ denotes the initial wave function, which is defined by the grating transmittance and assumed to be of the form

$$\psi(\xi',\zeta=0)=\sum_{j=-\infty}^{\infty}\delta(j-\xi'/2\pi). \tag{B3}$$

This distribution, sometimes referred to as "Dirac's comb," can be (formally) rewritten in terms of its Fourier series expansion,

$$\psi(\xi',0)=\sum_{j=-\infty}^{\infty}e^{ij\xi'}. \tag{B4}$$

After introducing Eq. (B3) into the Fresnel-Kirchhoff formula (B2), one immediately obtains

$$\psi(\xi,\zeta>0)=\frac{2\pi}{\sqrt{i\pi 4\zeta}}\sum_{j=-\infty}^{\infty}\exp\left[i\frac{(2\pi j-\xi)^2}{4\zeta}\right]. \tag{B5}$$

Introducing Eq. (B4) into the propagator (B2) and performing the Gaussian integrals, one obtains

$$\psi(\xi,\zeta\geqslant 0)=\sum_{j=-\infty}^{\infty}e^{ij\xi}e^{-ij^2\zeta}. \tag{B6}$$

As much as the dependence on j is concerned, both expressions are essentially of the same form and lead to the revival dynamics already described in the main part of the paper. By again choosing $\zeta=2\pi m/n$, where m and $n\neq 0$ are (positive) integers, and then introducing Eq. (3) into Eq. (B6), one finds

$$\psi\left(\xi,\zeta=2\pi\frac{m}{n}\right)=\sum_{r=1}^{n}C(r,m,n)\sum_{j=-\infty}^{\infty}\delta\left(j-\frac{\xi}{2\pi}-\frac{r}{n}\right). \tag{B7}$$

By proceeding the same way with Eq. (B5), one equivalently obtains

$$\psi\left(\xi,\zeta=2\pi\frac{m}{n}\right)=\sqrt{\frac{2m}{n}}e^{-i\pi/4}\exp\left(i\frac{n}{8\pi m}\xi^2\right)\times\sum_{r=1}^{4m}C^*(r,n,4m)\times\sum_{j=-\infty}^{\infty}\delta\left(\frac{2mj}{n}-\frac{\xi}{2\pi}-\frac{r}{2n}\right). \tag{B8}$$

We identify the corresponding δ peaks in Eqs. (B7) and (B8), and infer that $C(r,n,4m)=0$ for any odd r. Making use of this property, Eq. (B8) can be rewritten

$$\psi\left(\xi,\zeta=2\pi\frac{m}{n}\right)=\sqrt{\frac{2m}{n}}e^{-i\pi/4}\exp\left(i\frac{n}{8\pi m}\xi^2\right)\times\sum_{r=1}^{2m}C^*(2r,n,4m)\times\sum_{j=-\infty}^{\infty}\delta\left(\frac{2mj}{n}-\frac{\xi}{2\pi}-\frac{r}{n}\right), \tag{B9}$$

thus allowing a more direct comparison with Eq. (B7). Noticing that every pair of indices (r,j) is responsible for exactly *one* peak of the wave function, we arrive at

$$e^{-i\pi/4}\exp\left[i2\pi\frac{(r-2mj)^2}{4mn}\right]\sqrt{\frac{2m}{n}}C^*(2r,n,4m)=C(r+j[n-2m],m,n). \tag{B10}$$

Setting $(r,j)=(2m,1)$ and using the Talbot coefficient definition (4), this identity reduces to the Landsberg-Schaar formula (B1).

[1] M. V. Berry and M. Wilkinson, Proc. R. Soc. London, Ser. A **392**, 15 (1984).
[2] R. L. Liboff, Q. Appl. Math. **60**, 75 (2002).
[3] R. L. Liboff, Phys. Lett. A **269**, 230 (2000).
[4] H.-J. Stöckmann, J. Mod. Opt. **49**, 2045 (2002).
[5] A. P. Micolich, R. P. Taylor, R. Newbury, C. P. Dettmann, and T. M. Fromhold, Aust. J. Phys. **51**, 547 (1998).
[6] A. Kaplan, N. Friedman, M. Andersen, and N. Davidson, Phys. Rev. Lett. **87**, 274101 (2001).
[7] R. W. Robinett, Phys. Rep. **392**, 1 (2004).
[8] B. Rohwedder, Europhys. Lett. **60**, 505 (2002).
[9] D. C. Chang and E. F. Kuester, IEEE Trans. Microwave Theory Tech. **29**, 923 (1981).
[10] This is an example of a "discrete Fourier transform." The validity of Eq. (3) can be verified simply by introducing definition (4) and then applying the sum formula for geometric series.
[11] F. Gori, D. Ambrosini, R. Borghi, V. Mussi, and M. Santarsiero, Eur. J. Phys. **22**, 53 (2001).
[12] D. F. Styer, Am. J. Phys. **69**, 56 (2001).
[13] C. Jung, Can. J. Phys. **58**, 719 (1980).
[14] M. Pinsky, SIAM J. Math. Anal. **11**, 819 (1980).
[15] M. Pinsky, SIAM J. Math. Anal. **16**, 848 (1985).
[16] M. A. Doncheski and R. W. Robinett, Ann. Phys. **299**, 208 (2002).
[17] P. J. Richens and M. V. Berry, Physica D **2**, 495 (1981).
[18] R. L. Liboff and J. Greenberg, J. Stat. Phys. **105**, 389 (2001).
[19] There always exist wave functions that periodically revive. Here we are not talking about the periodic behavior of a set of particular wave functions, though, but about the intrinsically periodic behavior of certain quantum mechanical systems.
[20] V. Amar, M. Pauri, and A. Scotti, J. Math. Phys. **32**, 2442 (1991).
[21] V. Amar, M. Pauri, and A. Scotti, J. Math. Phys. **34**, 3343 (1993).
[22] P. Stifter, C. Leichtle, W. P. Schleich, and J. Marklof, Z. Naturforsch., A: Phys. Sci. **52**, 377 (1997).
[23] M. Wilkens, E. Goldstein, B. Taylor, and P. Meystre, Phys. Rev. A **47**, 2366 (1993).
[24] R. J. Cook and R. K. Hill, Opt. Commun. **43**, 258 (1982).
[25] V. Milner, J. L. Hanssen, W. C. Campbell, and M. G. Raizen, Phys. Rev. Lett. **86**, 1514 (2001).
[26] N. Friedman, A. Kaplan, D. Carasso, and N. Davidson, Phys. Rev. Lett. **86**, 1518 (2001).
[27] Yu. B. Ovchinnikov, S. V. Shul'ga, and V. I. Balykin, J. Phys. B **24**, 3173 (1991).
[28] H. Gauck, M. Hartl, D. Schneble, H. Schnitzler, T. Pfau, and J. Mlynek, Phys. Rev. Lett. **81**, 5298 (1998).
[29] Yu. B. Ovchinnikov, I. Manek, and R. Grimm, Phys. Rev. Lett. **79**, 2225 (1997).
[30] H. J. Lee, C. S. Adams, M. Kasevich, and S. Chu, Phys. Rev. Lett. **76**, 2658 (1996).
[31] R. Ozeri, L. Khaykovich, N. Friedman, and N. Davidson, J. Opt. Soc. Am. B **17**, 1113 (2000).
[32] M. F. Andersen, A. Kaplan, N. Friedman, and N. Davidson, J. Phys. B **35**, 2183 (2002).
[33] G. Chen, D. A. Church, B.-G. Englert, C. Henkel, B. Rohwedder, M. O. Scully, and M. Suhail Zubairy, *Quantum Computing Devices: Principles, Designs, and Analysis* (Chapman & Hall/CRC, New York, 2007).
[34] T. Schumm, S. Hofferberth, L. M. Andersson, S. Wildermuth, S. Groth, I. Bar-Joseph, J. Schmiedmayer, and P. Krüger, Nat. Phys. **1**, 57 (2005).
[35] D. Cassettari, B. Hessmo, R. Folman, T. Maier, and J. Schmiedmayer, Phys. Rev. Lett. **85**, 5483 (2000).
[36] W. Hänsel, J. Reichel, P. Hommelhoff, and T. W. Hänsch, Phys. Rev. A **64**, 063607 (2001).
[37] D. Jaksch, J. I. Cirac, P. Zoller, S. L. Rolston, R. Côté, and M. D. Lukin, Phys. Rev. Lett. **85**, 2208 (2000).
[38] A. Derevianko and C. C. Cannon, Phys. Rev. A **70**, 062319 (2004).
[39] S. Kuhr, W. Alt, D. Schrader, M. Müller, V. Gomer, and D. Meschede, Science **293**, 278 (2001).
[40] S. Kuhr, W. Alt, D. Schrader, I. Dotsenko, Y. Miroshnychenko, W. Rosenfeld, M. Khudaverdyan, V. Gomer, A. Rauschenbeutel, and D. Meschede, Phys. Rev. Lett. **91**, 213002 (2003).
[41] J. Ruostekoski, B. Kneer, and W. P. Schleich, and G. Rempe, Phys. Rev. A **63**, 043613 (2001).
[42] W. Zhang, E. M. Wright, H. Pu, and P. Meystre, Phys. Rev. A **68**, 023605 (2003).
[43] R. P. Taylor, A. P. Micolich, R. Newbury, T. M. Fromhold, A. Ehlert, A. G. Davies, L. D. Macks, C. R. Tench, J. P. Bird, H. Linke, W. R. Tribe, E. H. Linfield, and D. A. Ritchie, Phys. Scr., T **90**, 41 (2001).
[44] H.-J. Stöckmann, Phys. Bl. **53**, 121 (1997).
[45] N. Friedman, L. Khaykovich, R. Ozeri, and N. Davidson, Phys. Rev. A **61**, 031403(R) (2000).
[46] A. P. Itin, A. I. Neishtadt, and A. A. Vasiliev, Phys. Lett. A **291**, 133 (2001).
[47] S. Aubin, S. Myrskog, M. H. T. Extavour, L. J. LeBlanc, D. McKay, A. Stummer, and J. H. Thywissen, Nat. Phys. **2**, 384 (2006).
[48] F. Miao, S. Wijeratne, Y. Zhang, U. C. Corkum, W. Bao, and C. N. Lau, Science **317**, 1530 (2007).
[49] V. Arrizón and J. G. Ibarra, Opt. Lett. **21**, 378 (1996).
[50] B. Rohwedder, Fortschr. Phys. **47**, 883 (1999).
[51] E. E. Grigor'eva and A. T. Semenov, Sov. J. Quantum Electron. **8**, 1063 (1978).
[52] D. L. Aronstein and C. R. Stroud, Phys. Rev. A **55**, 4526 (1997).
[53] M. V. Berry and S. Klein, J. Mod. Opt. **43**, 2139 (1996).
[54] F. Gori, in *Current Trends in Optics*, edited by J. C. Dainty (Academic, San Diego, CA, 1994), Vol. 2, pp. 139–148.
[55] W. D. Montgomery, J. Opt. Soc. Am. **57**, 772 (1967).
[56] A. P. Smirnov, Opt. Spectrosc. **43**, 446 (1977).
[57] R. E. Ioseliani, Opt. Spectrosc. **55**, 544 (1983).
[58] E. T. Burtt and W. T. Catton, Proc. R. Soc. London, Ser. B **157**, 53 (1962).
[59] G. L. Rogers, Br. J. Appl. Phys. **15**, 594 (1964).
[60] U. Drodofsky, J. Stuhler, T. Schulze, M. Drewsen, B. Brezger, T. Pfau, and J. Mlynek, Appl. Phys. B: Lasers Opt. **65**, 755 (1997).
[61] B. Rohwedder, Am. J. Phys. **75**, 394 (2007).
[62] T. M. Apostol, *Introduction to Analytic Number Theory* (Springer, New York, 1976).
[63] V. Armitage and A. Rogers, J. Phys. A **33**, 5993 (2000).